actuating angle commands of fins, (X_M, Y_M, Z_M), (U,V,W), (P_f, Q_f, R_f), (ϕ_f, θ_f, ψ_f) are vehicle positions, velocities, angular rates, and attitudes; respectively. The output commands ($\delta_{1c}, \delta_{2c}, \delta_{3c}, \delta_{4c}$) are manipulated from mission planning, guidance laws and control laws with measured datum.

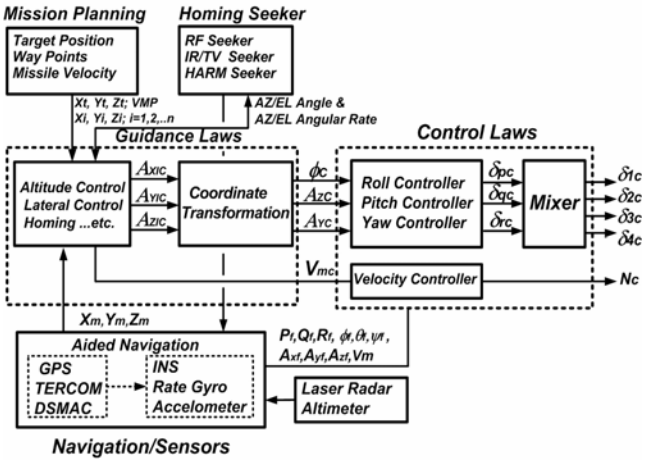

Fig.7. A typical guidance and control block diagram

5.2. Vertical and lateral mid-course guidance laws

There are two guidance laws for vertical and lateral planes in mid-course phase. The vertical guidance law can be implemented by the altitude control. The lateral guidance law can be implemented by the locus-tracking control. The control configurations are shown in Fig.8. Neglecting nonlinearities shown in Fig.8, output commands ($A_{ZIC}, A_{XIC}, A_{YIC}$) are

$$A_{ZIC} = [-(-Z_C + Z_M)k_{oz}C_{OZ}(s) + \dot{Z}_M]k_{iz}C_{IZ}(s) - g \quad (55)$$

$$A_{XY} = [(L_C - L_M)k_{ol}C_{OL}(s) - \dot{L}_M]k_{il}C_{IL}(s) \quad (56)$$

$$A_{XIC} = -A_{XY}\sin(\psi) \quad (57)$$

$$A_{YIC} = +A_{XY}\cos(\psi) \quad (58)$$

where Z_C is the altitude command; Z_M is the measured altitude, and $\dot{Z}_M$ is the derivative of Z_M; L_C is the locus tracking command; L_M is the calculated data, and $\dot{L}_M$ is the derivative of L_M. Nonlinearities include output command limitations ($A_{XLIM}, A_{YLIM}, A_{ZLIM}$), output command-rate limitations (H_{DLIM}, L_{DLIM}), and command tracking error shaping.

The concepts of locus tracking are shown in Fig.9. The tracking locus connected with waypoint # i (X_i, Y_i) and way point #i+1 (X_{i+1}, Y_{i+1}) and tracking definition is formulated as following equations. The tracking locus is defined as

$$a_{i+1}X + b_{i+1}Y + c_{i+1} = 0 \quad (59)$$

where $a_{i+1} = Y_{i+1} - Y_i, b_{i+1} = X_{i+1} - X_i$ *and* $c_{i+1} = X_iY_{i+1} + X_{i+1}Y_i$, the normal displacement between vehicle (X_m, Y_m) and the tracking locus is

$$L_M = -(a_{i+1}X_m - b_{i+1}Y_m + c_{i+1})/\sqrt{a_{i+1}^2 + b_{i+1}^2} \quad (60)$$

Positive value of L_M represents the vehicle is on the right-hand side of the tracking locus; negative value of L_M represents the vehicle is on the left-hand side of the tracking locus. The purpose of locus tracking is to keep L_M be a wanted value (L_C); and moving from point #i toward point #i+1. L_C =0 represents the vehicle will moving on the tracking locus. The R_{CTLi} is range to way point #i in which the tracking loci is changed to L_{i+1}. It is used for smoothing the flight locus. It is function of turning angle ψ_{ci} between tracking locus L_{i1} and L_{i+1}. In this work, R_{CTLi} is evaluated as

$$R_{CTLi} = 2500[1 + |\psi_{ci}|/90] \quad (61)$$

for $V_M = 238m/s$ and the maximal lateral manoeuvre is limited to be $17.32m/s^2$. Note that vertical and lateral mid-course guidance laws are analyzed and designed by linear control theorem.

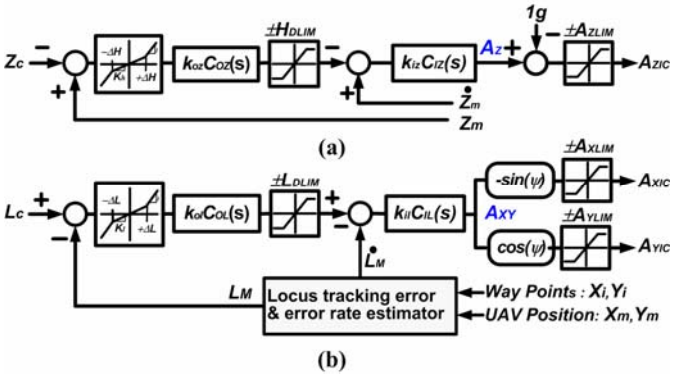

Fig.8. Guidance laws of (a) vertical plane and (b) horizontal plane.

5.3 2D terminal homing guidance laws

The line of sights between vehicle (X_M, Y_M, Z_M) and target (X_T, Y_T, Z_T) are

$$\psi_T = 57.3 \tan 2^{-1}(Y_T - Y_M, X_T - X_M) \quad (62)$$

and

$$\theta_T = 57.3 \tan 2^{-1}(Z_T - Z_M, X_T - X_M) \quad (63)$$

The line of sight rates ($\dot{\psi}_T, \dot{\theta}_T$) are manipulated by the following filter

$$D_{sk}(s) = sW_{SK} /(s + W_{SK}) \quad (64)$$

The value of W_{SK} is chosen as 16rad/sec. The vertical and lateral commands are evaluated from proportional navigation methods. They are given below:

$$A_{ZIC} = N_Z V_C \dot{\theta}_T - g \quad (65)$$

$$A_{XY} = N_Y V_C \dot{\psi}_T \quad (66)$$

$$A_{XIC} = -A_{XY} \times \sin(\psi) \quad (67)$$

$$A_{YIC} = A_{XY} \cos(\psi) \quad (68)$$

where V_C is the approaching speed between vehicle and target. N_Y and N_Z are proportional navigation constants. Their values are chosen as 1.0 and 0.2 for low altitude control and large lateral manoeuvre.

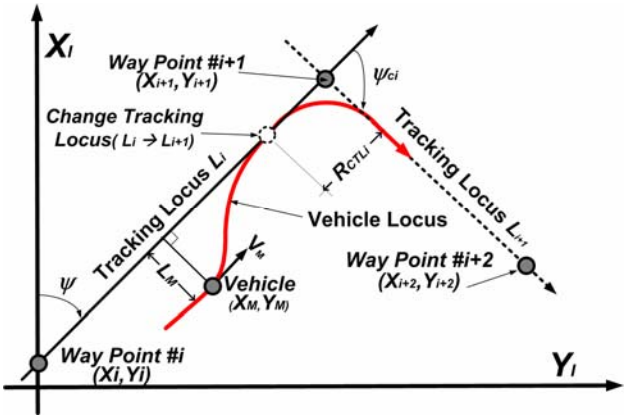

Fig.9. Lateral locus tracking concept.

5.4 Guidance Command Transformations

Guidance commands ($A_{XIC}, A_{YIC}, A_{ZIC}$) evaluated from Eqs(55)-(58) and Eqs(65)-(68) represent the commands in the inertial reference axes[12,13]. They are outputs of altitude, lateral and homing larws of 2D terminal homing guidance laws. They must be transferred into body-axis commands (ϕ_C, A_{ZC}, A_{YC}) . The transformation is dependent on STT or BTT maneuver used:

(a)The command tranformation for STT maneuver

$$\begin{bmatrix} A_{XC} \\ A_{YC} \\ A_{ZC} \end{bmatrix} \equiv \begin{bmatrix} c\theta c\psi & s\phi s\theta c\psi - c\phi s\psi & c\phi s\theta c\psi + s\phi s\psi \\ c\theta s\psi & c\phi c\psi + s\phi s\theta s\psi & c\phi s\theta s\psi - s\phi c\psi \\ -s\theta & s\phi c\theta & c\phi c\theta \end{bmatrix}^{-1} \begin{bmatrix} A_{XIC} \\ A_{YIC} \\ A_{ZIC} \end{bmatrix} \quad (69)$$

where $c\bullet = cos(\bullet)$, $s\bullet = sin(\bullet)$

The A_{XC} is used for speed control, and (A_{YC}, A_{ZC}) are used for yawing and pitching controls. The rolling angular command ϕ_c is set to be zero. Fig.3 shows the maneuverbility on yaw-axis is limited. Therefore, STT maneuver is used for small A_{YC} only.

(b)The command tranformation for BTT manuver

The guidance commands on inertial axes are first transferred to body axes

$$\begin{bmatrix} A_{XB1} \\ A_{YB1} \\ A_{ZB1} \end{bmatrix} \equiv \begin{bmatrix} c\theta c\psi & s\phi s\theta c\psi - c\phi s\psi & c\phi s\theta c\psi + s\phi s\psi \\ c\theta s\psi & c\phi c\psi + s\phi s\theta s\psi & c\phi s\theta s\psi - s\phi c\psi \\ -s\theta & s\phi c\theta & c\phi c\theta \end{bmatrix}^{-1} \begin{bmatrix} A_{XIC} \\ A_{YIC} \\ A_{ZIC} \end{bmatrix} \quad (70)$$

for $\phi = 0°$. A_{XB1} is usually set to be zero for constant vehicle speed. A_{ZB1} and A_{YB1} are further distributed from bank angle ϕ_c and acceleration command A_{ZC} . They are

$$A_{ZC} = -A_{ZBCO}, \phi_c = -\phi_{co}, \ for \ A_{ZB1} < 0 \ and \ A_{YB1} < 0 \quad (71)$$

$$A_{ZC} = -A_{ZBCO}, \phi_c = +\phi_{co}, \ for \ A_{ZB1} < 0 \ and \ A_{YB1} \geq 0 \quad (72)$$

$$A_{ZC} = +A_{ZBCO}, \phi_c = -\phi_{co}, \ for \ A_{ZB1} \geq 0 \ and \ A_{YB1} \geq 0 \quad (73)$$

$$A_{ZC} = +A_{ZBCO}, \phi_c = +\phi_{co}, \ for \ A_{ZB1} \geq 0 \ and \ A_{YB1} < 0 \quad (74)$$

where

$$A_{ZBCO} = \sqrt{A_{ZB1}^2 + A_{YB1}^2} \ (\text{m/s})$$

$$\phi_{co} = 57.3 \tan 2^{-1}(|A_{YB1}|, |A_{ZB1}|) \ (\text{deg}).$$

The command A_{YC} on the yawing channel is set to be zero for BTT maneuver.

5.5. STT and BTT switching logic

The switching criterion is dependent on the value of horizontal command A_{XY} described by Eqs.(56) and (66). In this work, BTT manoeuvre is used for $|A_{XY}|$ is greater than $2.5 m/s^2$.

6.Simplified equations of motion with found aerodynamic coefficients

6.1 Block diagrams of 6-DOF Simulation

Fig.10 shows the simulation block diagram of the UAV, in which $(\delta_{1c},\delta_{2c},\delta_{3c},\delta_{4c})$ *are* four actuating command of fins, (X,Y,Z) , (U,V,W) , (P,Q,R) , (ϕ,θ,ψ) are positions, velocities, angular rates, and attitudes; respectively. $(X,Y,Z),(U,V,W)$, $(\dot{P},\dot{Q},\dot{R})$, $(\dot{\phi},\dot{\theta},\dot{\psi})$ are derivatives of (X,Y,Z), $(U,V,W),(P,Q,R),(\phi,\theta,\psi)$, $(\dot{U},\dot{V},\dot{W})$, $(\dot{P},\dot{Q},\dot{R})$ are represented by Eqs.(1)-(6). The relationship between them will be discussed in the next subsections. Solutions of the ordinary differential equations(ODE) are solved by Runge-Kutta Method[14].

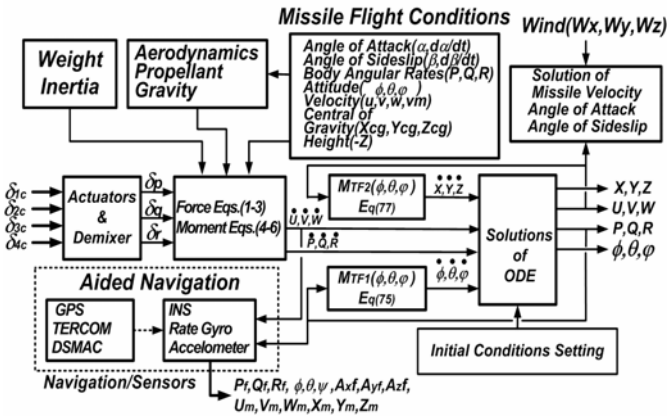

Fig.10. Simulation block diagram of the AUV.

6.2. Kinematics of the UAV

The kinematics of the UAV including transformations of body angular rates to attitude angle, forces to derivatives of velocities, and derivatives of velocities to derivatives of positions. They are given below:

(1)Transformation from body angular rate (P,Q,R) to Euler angular rate $(\dot{\phi},\dot{\theta},\dot{\psi})$ is

$$\begin{bmatrix}\dot{\phi}\\ \dot{\theta}\\ \dot{\psi}\end{bmatrix}=\begin{bmatrix}1 & \sin\phi\tan\theta & \cos\phi\tan\theta\\ 0 & \cos\phi & -\sin\phi\\ 0 & \sin\phi\sec\theta & \cos\phi\sec\theta\end{bmatrix}\begin{bmatrix}P\\ Q\\ R\end{bmatrix} \quad (75)$$

The sequence of transformation is from yawing through pitching to rolling angles (i.e., $\psi\Rightarrow\theta\Rightarrow\phi$). The domain of yawing angle is $-180^\circ<\psi<+180^\circ$, pitching angle is $-90^\circ<\theta<+90^\circ$, and rolling angle is $-90^\circ<\phi<+90^\circ$. Therefore, there is a singularity at $\theta=90^\circ$ of Eq.(75) and it needs quatered element method for vertical launch. In this work, vertical lauch is avoided by small perturbed from $\theta=90^\circ$.Note that (P,Q,R) is the ODE solution of Eqs.(4)-(6).

(2)Transformation from gravital force(g), body accelerations (A_{XB},A_{YB},A_{ZB}) with body angular rates (P,Q,R) to deviation of body-axis velocity $(\dot{U},\dot{V},\dot{W})$ is

$$\begin{aligned}\dot{U}&=-QW+RV+A_{XB}-g\sin\theta\\ \dot{V}&=-RU+PW+A_{YB}+g\cos\theta\sin\phi\\ \dot{W}&=QU-PV+A_{ZB}+g\cos\theta\cos\phi\end{aligned} \quad (76)$$

Equation (76) is rewriten from Eqs.(1)-(3).

(3)Transformation from three body-axis velocity commponests (U,V,W) to deviations of position components ($\dot{X},\dot{Y},\dot{Z}$).

$$\begin{bmatrix}\dot{X}\\ \dot{Y}\\ \dot{Z}\end{bmatrix}\equiv\begin{bmatrix}c\theta c\psi & s\phi s\theta c\psi-c\phi s\psi & c\phi s\theta c\psi+s\phi s\psi\\ c\theta s\psi & c\phi c\psi+s\phi s\theta s\psi & c\phi s\theta s\psi-s\phi c\psi\\ -s\theta & s\phi c\theta & c\phi c\theta\end{bmatrix}\begin{bmatrix}U\\ V\\ W\end{bmatrix} \quad (77)$$

where $c\bullet=cos(\bullet)$, $s\bullet=sin(\bullet)$

$(X,Y,Z),(U,V,W),(P,Q,R),(\phi,\theta,\psi)$ are found by solving ordinary differential equations(ODE) described by Eqs.(75)-(77) and Esq.(4)-(6). Note that (X_m,Y_m,Z_m) , (P_f,Q_f,R_f) , (ϕ_f,θ_f,ψ_f) represent the outputs of sensors. They used for guidance and controls.

6.3.The Simplified 6-DOD simulation models

In Section 2, small-signal perturbed aerodynamic model is developed form trim conditions. In Section 3, aerodynamic coefficients of the small-signal perturbed aerodynamic model are evaluated form flight identification procrsses. In Section 4,

autopilots can be found with design specifications and found aerodynamic coefficients. In this pararaph, the simplified 6-DOF simulation model is re-constructed from found aerodynamic coefficients with trim added back and gains of autopilots; i.e., combination of Figs.2 and 6[8]. Fig.11 shows the simulation block diagram. Note that compensators and dynamics of hardware are neglected for simplicity of this illustration. They will be included in flight simulation testing and given in Appendix A.

Aerodynamic coefficents shown in the right-hand side of Fig.11 are found in Section 3. Gravity(g), angle of attack($\tilde{\alpha}$), angle of sideslip($\tilde{\beta}$) are added to simulate Eqs.(1)-(6). Kinematic couplings $P\tan(\tilde{\beta})$ and $P\tan(\tilde{\alpha})$ are added. The term $(\theta-\alpha^T\cos(\phi))/2.0$ is used to correct the trim condition of the constant altitude flight. In this work, $\alpha^T=2.09°$ for $V_M=238m/s$. The angle of attack will be diverging without this correct term. This the major difference between the this paper and the Reference 8.

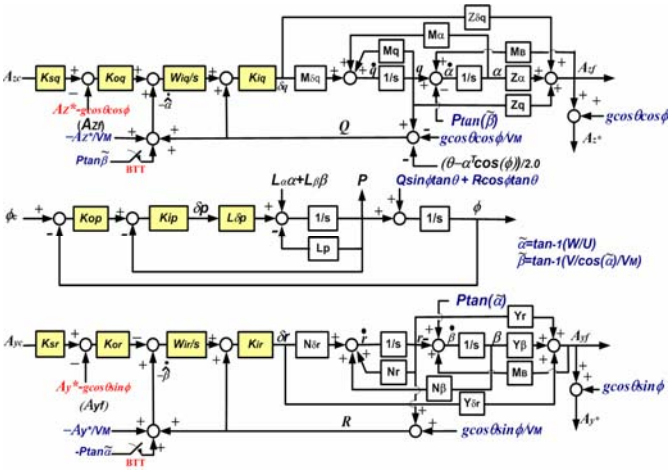

Fig.11. Simulation block diagrams of (a)pitching, (b)yawing, and (c) rolling channels.

7. Flight simulation verfications

7.1. Guidance and Control Law Designs

The control configuration of the autopilot is shown in Fig.6. Using the autopilot design procedure stated in Section 4, the found gains are given belows:

$$K_{sq}=1.0225, K_{oq}=0.0190, W_{iq}=4.362, K_{iq}=0.3769$$

for $T_q=0.244, \zeta_q=0.75, \omega_q=8.044, \omega_{zq}=10.52$, and

$$K_{sr}=1.005, K_{or}=0.09715, W_{ir}=4.0216, K_{ir}=0.5057$$

for $T_r=0.252, \zeta_r=1.10\ \omega_r=7.159, \omega_{zr}=7.635$, and

K_{op}=6.28;K_{ip}=0.1104.

The parameters shown in Fig.8 are given belows:

$$k_{oz}=0.75; k_{iz}=1.00; k_{ol}=0.75; k_{il}=1.00$$

The suitability of design parameters is verified by 6-DOF simulations.

7.2 Flight Simulation Verifications

Figs.12-14 show comparisons between simplified and completed models used in 6-DOF simulations. Fig.12 shows the flight loci, Fig.13 shows guidance commands, and Fig.14 shows attirudes of the UAV. Comparison results give the simplified 6-DOF models can replace the completed 6-DOF models. Fig.15 shows pitching angles for (1)flight datum; (2)proposed method; and (3) no kinmatic and correct terms added(Ref.8). It can be seen that the proposed method gives good approximation to the flight datum; i.e., accurate trim condition.

8. Conclusions

In this paper, aerodynamic modeling, identification processes and the simplified 6-DOF model have been evaluated and proposed for an unmaned unmanned aerial vehicle(UAV). The evaluation procedures were illustrated by a Tomahawk-like cruise unmanned vehicle. Simulation verification results have shown that it gave good approximation for completed 6-DOF simulation model; and gave more accurate simulation model for pitch angle and angle of attack than previous paper developed by the author[8].

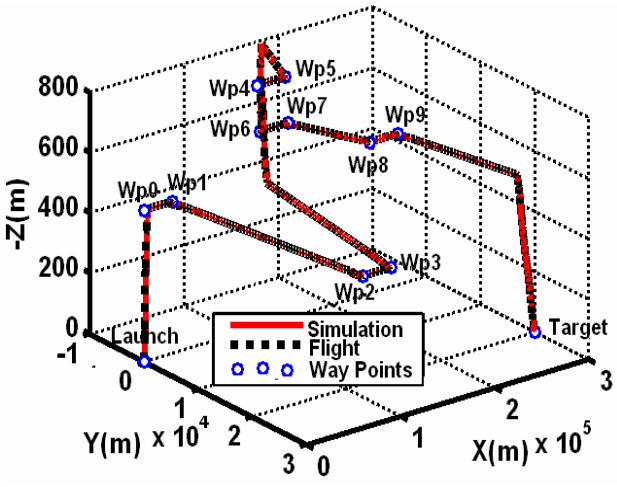

Fig.12. Flight Loci.

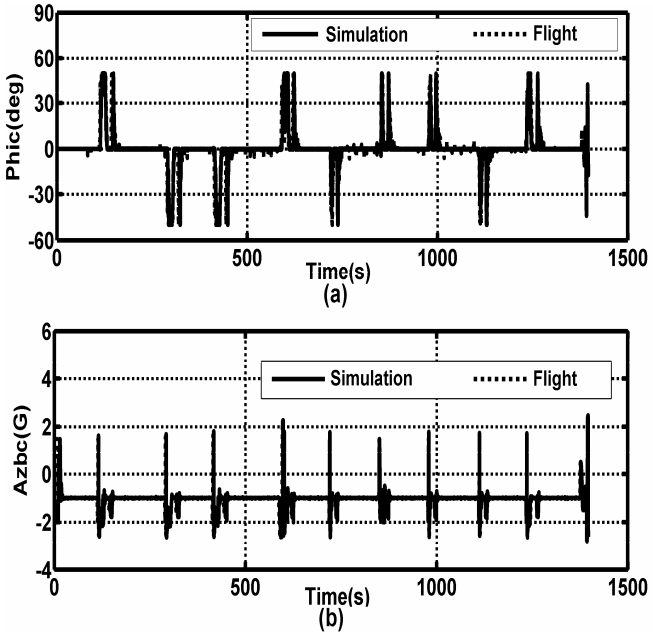

Fig.13. Guidance Commands (a) ϕ_c ; (b) Azc

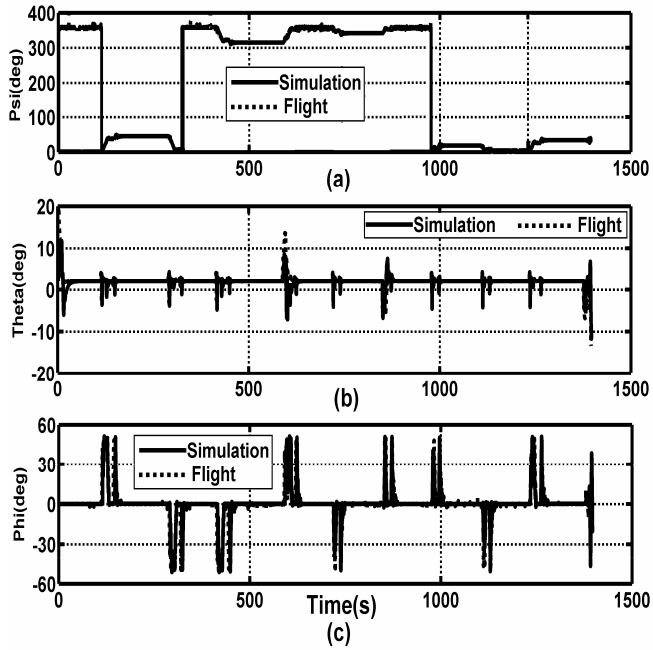

Fig.14. Attitudes of UAV(a) ψ_f ,(b) θ_f ,(c) ϕ_f .

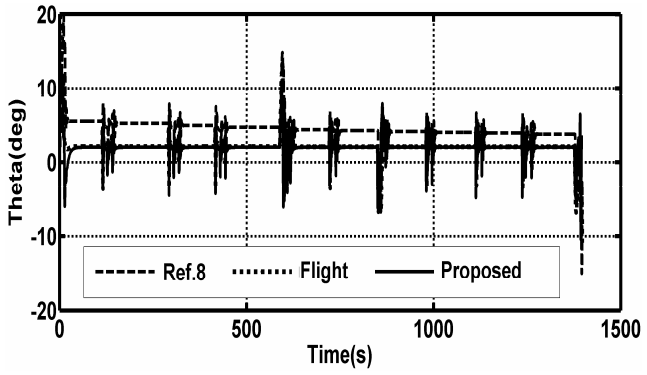

Fig.15. Comparisons of Pitching Angles.

References:

[1].Salman, S. A., Sreenatha, A. G., and Choi, J.Y., Attitude Identification of Unmaned Aircraft Vehicle, International Journal of Control, Automation and Systems, Vol.4, No.6, 2006, pp.782-787.

[2].Lyshevski, S. E., Identification of nonlinear flight dynamics: Theory and practice, IEEE Trans. on Aerospace and Electronic Systems, Vol. 36, No. 2, 2000, pp. 383-392.

[3].Weiss, M., Bucco, D., Handover analysis for tactical guided weapons using the adjoin method, AIAA Guidance, Navigation and Control Conference, 15 - 18 August 2005, San Francisco, California.

[4].Gilks, W. R., Richardson, S., and Spiegelhalter, D. J., Markov Chain Monte Carlo in Practice. Boca Raton, FL: Chapman & Hall, 1996.

[5].Nesline, F. W. and Zarchan, P., Robust Instrumentation Configurations for Homing Missile Flight Control, AIAA Guidance Control Conference, AIAA-Paper-80-1749, 1980, pp.209- 219.

[6].Nesline, F. W. and Nesline, M.L., How Autopilot Requirements Constraint the Aerodynamic Design of Homing Missile, American Control Conference, , pp.716-730 1984.

[7].Blakelack, J. H., Automatic Control of Aircraft and Missile, Second Edition, John Wiley and Sons, New York, 1991.

[8].Tsay, T. S., Simplified 6-DOF Simulation Models and Guidance Laws for Bank to Turn Unmanned Aerial Vehicles, Journal of Formosa University, Vol.27, No.2, 2008, pp.11-26.

[9].McLean, D., Automatic Flight Control System, Prentice Hall, 1990.

[10].Tomahawk Land Attack Operational Flight Software Engineering Design Analysis, T-SMB-0084-00, 1983.

[11].Macknight, N., Tomahawk Cruise Missile, Motorbooks, 1995

[12].Cochran, T. S., Jr. J. E., Kim, J-K, and Kim, E. G. A Design Method for Guidance Laws for Bank-To-Turn Missiles, Journal of Guidance, Control, and Dynamics, Vol. 24, No. 2, 2001, pp. 255-260.

[13].Fu, L.-C., Chang, W.-D. Yang, J.-H. and Kuo, T.-S., Adaptive Robust Bank-to-Turn Missile Autopilot Design Using Neural Networks, AIAA Journal of Control, Guidance, and Dynamics, Vol. 20, No. 2, 1997, pp. 346-354.

[14].Butcher, J. C., *Numerical methods for ordinary differential equations*. John Wiley & Sons, 2003.

Appendix A: Compensators and Hardware dynamics

The dynamics of hardware and compensators are given bellows:

1.Actuator dynamics

$$T_{CAS}(s)=\frac{986}{s^2+37.68s+986}$$

2.Accelerometer dynamics and low-pass filter

$$T_{ACC}(s)=\frac{193444}{s^2+263.9s+193444}$$

$$T_{LPFO}(s)=\frac{188.5}{s+188.5}$$

3.Rate gyro dynamics and low-pass filter

$$T_{RG}(s)=\frac{193444}{s^2+263.9s+193444}$$

$$T_{LPFI}(s)=\frac{314.2}{s+314.2}$$

4.Compensators of vertical and lateral guidance laws

$$C_{OZ}(s)=\frac{1/0.628s+1}{1/6.28s+1};C_{IZ}(s)=\frac{1/3.14s+1}{1/31.4s+1};$$
$$\Delta_H=35;k_1=0.5;k_2=1$$
$$C_{OL}(s)=\frac{1/0.628s+1}{1/6.28s+1};C_{IL}(s)=\frac{1/3.14s+1}{157s+1};$$
$$\Delta_L=150;k_1=0.5;k_2=1;$$

5. Compensators of rolling/pitching/yawing autopilots

$$P_{OC}(s)=\frac{1/23.48s+1}{1/18.14s+1};P_{IC}(s)=\frac{1/35s+1}{1/117.4s+1}$$
$$Q_{OC}(s)=\frac{1/39s+1}{1/13s+1};Q_{IC}(s)=\frac{1/20.1s+1}{1/62.8s+1}$$
$$R_{OC}(s)=\frac{1/20s+1}{1/5s+1};R_{IC}(s)=\frac{1/25.12s+1}{1/75.36s+1}$$